

Electroweak and Top Physics at the Tevatron and Indirect Higgs Limits

Sandra Leone¹ ^a(for the CDF and D0 Collaborations)

INFN Sezione di Pisa (Italy)

Abstract. We report a selection of the most recent CDF and D0 results on top quark and W and Z boson properties, based on Tevatron Run 2 data. The large datasets of W and Z bosons allow a very precise measurement of the W mass and detailed studies of vector boson production and asymmetries. Associated production of vector boson pairs has been observed and cross sections have been measured. The top quark is being studied in great detail, and a precision of 1.1% in the measurement of its mass has been achieved. The precise knowledge of top and W masses are constraining the allowed mass range of a standard model Higgs in an unprecedented way.

PACS. 14.70.Fm W bosons – 14.70.Hp Z bosons – 14.65.Ha Top quarks – 14.80.Bn Standard-model Higgs bosons

1 Introduction

The CDF and D0 experiments are multipurpose detectors taking data at the Tevatron Collider. The Tevatron provides proton-antiproton collisions at a center-of-mass energy $\sqrt{s} = 1.96$ TeV. In 2001 the Tevatron Run 2 began, after a five year period of significant upgrade of the accelerator itself and of the CDF and D0 experiments. Accelerator performances have kept improving since the start of Run 2. A peak luminosity of $2.92 \times 10^{32} \text{ cm}^{-2}\text{s}^{-1}$ has been recently achieved, and more than 3 fb^{-1} of integrated luminosity has been delivered so far to both experiments. The detectors collect data with an average efficiency of about 85%. As of these proceedings, $\simeq 2.5 \text{ fb}^{-1}$ were written to tape by each experiment.

A description of the CDF and D0 upgraded detectors can be found in [1].

2 W and Z Cross Section Measurements

W and Z bosons are produced at the Tevatron through $q\bar{q}$ annihilation and are identified by their leptonic decay into electrons, muons and taus. The signature is given by high energy charged leptons and high missing transverse energy for W candidates and two oppositely charged high energy leptons for Z candidates. W and Z identification is a key ingredient for top physics. W and Z boson decays are often components of background in searches for processes beyond the standard model (SM) and, being relatively well known processes, are used for calibrations and detector checks.

The samples of W and Z boson decays collected by CDF and D0 now number in the millions of events, and have been used to produce excellent measurements of electroweak observables.

Inclusive cross sections of both W and Z production have been measured in all the three lepton decay channels [2]. All measurements are in agreement with the NNLO calculations [3]. The accuracy is limited by systematic effects (dominated by the luminosity uncertainty of 6%).

The large statistics collected allows CDF to produce a $d\sigma(Z)/dy$ measurement for $Z^0/\gamma^* \rightarrow e^+e^-$ events obtained from 1.1 fb^{-1} of data. Figure 1 shows the $d\sigma(Z)/dy$ distribution compared to theory prediction. The total cross section integrated over all dielectron rapidities is $\sigma(Z) = 263.34 \pm 0.93(\text{stat}) \pm 3.79(\text{syst}) \text{ pb}$. This measurement, with increased statistics, can be used to constrain the parton distribution functions (PDFs).

Recently, CDF measured the ratio R of central-to-forward cross sections for $p\bar{p} \rightarrow W \rightarrow e\nu$ and obtained $R = 0.925 \pm 0.033$ [4]. The largest experimental uncertainty, due to luminosity, cancels in this ratio. The measurement can be compared to theoretical predictions obtained using different PDFs (see Fig. 2). This quantity is sensitive to the W rapidity distribution, and provides a novel way to constrain the PDFs.

3 W Mass Measurement

The W mass (M_W) is measured in the $e\nu$ and $\mu\nu$ channels from a maximum likelihood fit to the lepton transverse momentum and the transverse mass spectrum,

^a Email: sandra.leone@pi.infn.it

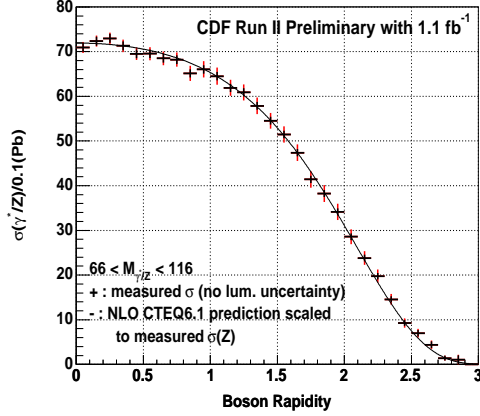


Fig. 1. The measured $d\sigma/dy$ (crosses) compared to theory prediction (solid line) for $Z \rightarrow e^+e^-$.

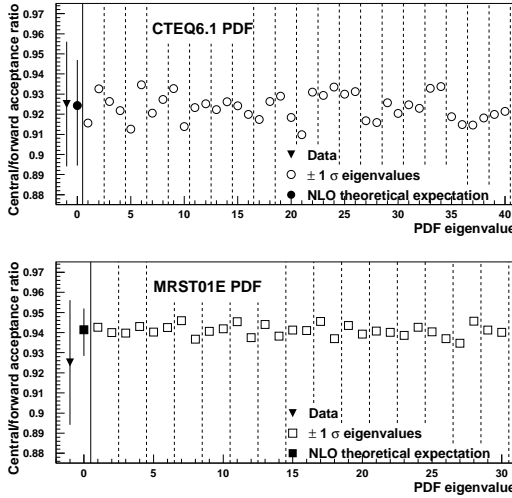


Fig. 2. CDF experimental ratio of central-to-forward cross sections (solid triangles) compared to the CTEQ6.1 (upper plot) and MRST01E (lower plot) acceptance ratios (solid circles and squares). Dashed lines separate PDF eigenvectors.

defined as:

$$M_T = \sqrt{2p_T^\ell p_T^\nu (1 - \cos \Delta\phi)},$$

where p_T is the lepton transverse momentum and $\Delta\phi$ is the difference in azimuthal angle between the two leptons. There are two main components leading to a precise M_W measurement: calibration of the detector to the highest possible precision and simulation of the p_T (M_T) spectrum. CDF measured the W mass using a sample of 200 pb^{-1} of electron and muon data, with the result: $M_W = 80413 \pm 34 \text{ (stat)} \pm 34 \text{ (syst)} \text{ MeV}/c^2 = 80413 \pm 48 \text{ MeV}/c^2$ [5]. This is the most precise single measurement of the W mass to date. The updated world average is $M_W = 80398 \pm 25 \text{ MeV}/c^2$ [5,6]. In Table 1 the various contributions to the systematic uncertainty are shown. The dominant uncertainties are due to the W boson statistics

Table 1. The uncertainties in MeV/c^2 on the M_T fit for M_W obtained from 200 pb^{-1} of CDF Run 2 data.

Uncertainty (MeV/c^2)	Electrons	Muons
Lepton scale	30	17
Lepton Resolution	9	3
Recoil Scale	9	9
Recoil Resolution	7	7
$u_{ }$ Efficiency	3	1
Lepton Removal	8	5
Backgrounds	8	9
$p_T(W)$	3	3
PDF	11	11
QED	11	12
Total systematic	39	27
Statistical	48	54
Total	62	60

and to the lepton energy scale calibration. They will be reduced with increased statistics in the W boson and calibration data samples. Since many simulation parameters are constrained by data control samples, their uncertainties are statistical and are expected to be reduced with more data as well. By the end of Run 2 the Tevatron experiments should be able to reduce the uncertainty on M_W below $20 \text{ MeV}/c^2$.

4 Direct W Width Measurement

CDF and D0 measured directly the W boson width Γ_W using the high tail of the M_T distribution. The width is determined by normalizing the predicted signal and background M_T distribution in the region of $50 < M_T < 90 \text{ GeV}/c^2$ and then fitting the predicted shape of the candidate events in the tail region $90 < M_T < 200 \text{ GeV}/c^2$ which is most sensitive to the width. CDF has the most precise measurement of this quantity, based on 350 pb^{-1} of data: $\Gamma_W = 2032 \pm 71 \text{ MeV}/c^2$, in good agreement with SM predictions [7]. Figure 3 shows the M_T distribution in the electron channel used for the Γ_W measurement. The updated world average is: $\Gamma_W = 2106 \pm 50 \text{ MeV}/c^2$ [7].

5 W Charge Asymmetry

W bosons at the Tevatron are primarily produced by annihilation of valence u (d) and anti- d (anti- u) quarks to W^+ (W^-). Since u quarks carry, on average, a higher fraction of the proton momentum than d quarks, a W^+ (W^-) tends to be boosted in the (anti-)proton direction. This results in a charge asymmetry defined as:

$$A_{y_W} = \frac{d\sigma(W^+)/dy_W - d\sigma(W^-)/dy_W}{d\sigma(W^+)/dy_W + d\sigma(W^-)/dy_W},$$

where y_W is the W rapidity and $d\sigma(W^\pm)/dy_W$ is the differential cross section for W^\pm production. A measurement of the charge asymmetry is sensitive to the

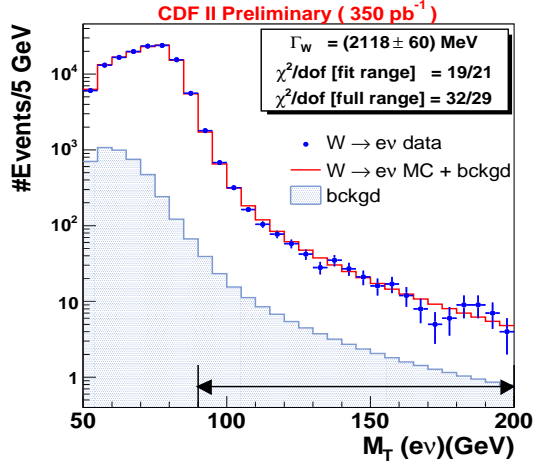


Fig. 3. The M_T fit for Γ_W in $W \rightarrow e\nu$ events. The fit is performed in the region 90–200 GeV.

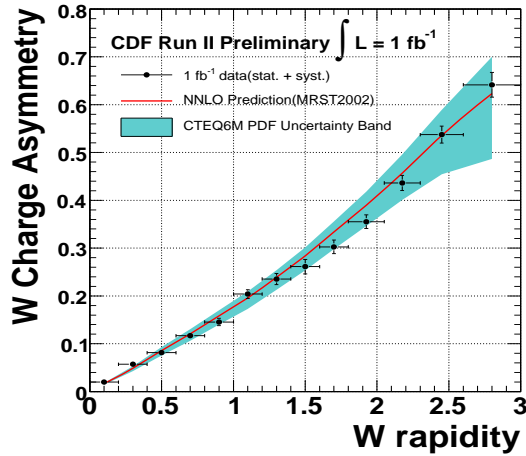


Fig. 4. Measured $A(|y_W|)$ compared to CTEQ5L prediction. The band illustrates the range of uncertainty on the CTEQ prediction.

ratio of u and d quark components of the PDFs. However, since the longitudinal component of the neutrino momentum is not measured, the asymmetry has been measured traditionally as:

$$A(\eta_e) = \frac{d\sigma(e^+)/d\eta_e - d\sigma(e^-)/d\eta_e}{d\sigma(e^+)/d\eta_e + d\sigma(e^-)/d\eta_e},$$

where η_e is the electron pseudorapidity. The observed asymmetry is a convolution of the W production charge asymmetry and the $V - A$ asymmetry of the W decay [8]. CDF has recently implemented a new analysis method that directly reconstructs y_W from $W \rightarrow e\nu$ events, using 1 fb^{-1} of data. The ambiguity due to the longitudinal neutrino component can be partly resolved on a statistical basis from the known $V - A$ decay distribution and $d\sigma(W^\pm)/dy_W$. Figure 4 shows the measured asymmetry as a function of y_W compared to the CTEQ5L PDF prediction.

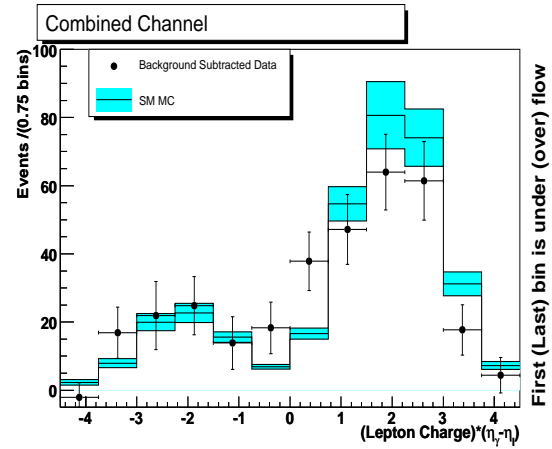


Fig. 5. D0 result for the charge-signed rapidity difference of $W\gamma$ candidates, after background subtraction.

6 Diboson Production

The SM implies that the electroweak gauge bosons W and Z can interact with one another through trilinear and quartic gauge boson vertices. Study of events containing pairs of vector bosons provides a sensitive test of the SM since physics beyond the SM could alter the cross sections and the production kinematics. In addition, diboson production represents a test bed for search and detection of the Higgs boson.

All associated production processes involving pairs of W , Z and γ bosons have been detected, with cross sections in excellent agreement with SM predictions. Both CDF and D0 measured inclusive cross sections for WW production [9] and $Z\gamma$ production [10].

6.1 $W\gamma$ Radiation Amplitude Zero

The $W\gamma$ production can be used to study the gauge structure of the SM. The interference among the three tree-level diagrams involved in $W\gamma$ production creates a zero in the center-of-mass angular distribution θ^* between the W and the direction of the incoming quarks. D0 measures the charge-signed photon-lepton rapidity difference distribution, which is sensitive to the radiation amplitude zero. Figure 5 shows the charge-signed rapidity difference in both electron and muon channel, obtained by D0 using 900 pb^{-1} of data. The observed distribution is consistent with the SM prediction and has a shape indicative of the radiation amplitude zero, although the result is statistically limited.

6.2 WZ Production

At $\sqrt{s} = 1.96 \text{ TeV}$, the SM predicts $\sigma(WZ) = 3.7 \pm 0.25 \text{ pb}$ [11]. D0 recently updated on 1 fb^{-1} of data its previous evidence for WZ production in events with three charged leptons [12]. They measure $\sigma(WZ) = 2.7^{+1.7}_{-1.3} \text{ pb}$. In winter 2007 CDF presented the observation of the WZ process based on 1.1 fb^{-1} of data [13]. In this analysis a significant improvement

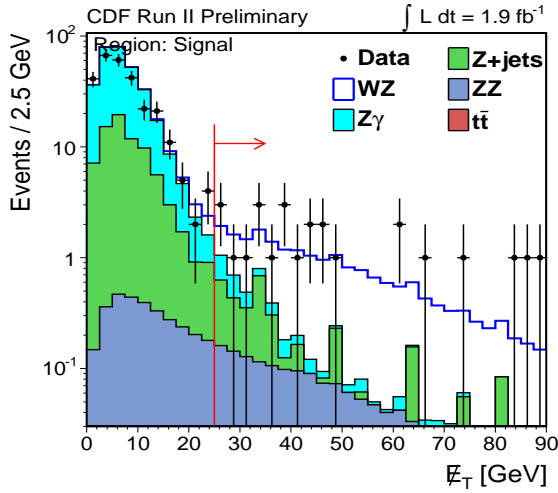


Fig. 6. Missing E_T distribution of WZ candidates compared to MC expectations. The arrow indicates the signal region.

was obtained by exploiting all the available detector information in defining leptons, therefore increasing the lepton acceptance. Recently CDF measurement was updated on 1.9 fb^{-1} of data. The measured cross section is $\sigma(WZ) = 4.3^{+1.4}_{-1.1} \text{ pb}$. Figure 6 shows the missing E_T distribution in the signal region.

6.3 ZZ Production

The ZZ production cross section predicted by the SM at the Tevatron is $\sigma(ZZ) = 1.4 \pm 0.1 \text{ pb}$ at NLO. D0 observed 1 candidate event and put an upper limit on the production cross section of $\sigma(ZZ) < 4.3 \text{ pb}$ at 95% C.L.. CDF combined the final states with 4 charged leptons and 2 charged leptons plus 2 neutrinos, and did a measurement of the ZZ production cross section $\sigma(ZZ) = 0.75^{+0.71}_{-0.54}$, based on 1.5 fb^{-1} of data. The observed signal has a significance of 3σ . This is the smallest cross section measured at the Tevatron. Figure 7 shows the likelihood ratio distribution for $ll\nu\nu$ candidate events.

7 Top Quark Physics

The top quark, discovered in 1995 at the Tevatron [14], has proven to be a very interesting particle. It is unique among known fermions because of its large mass, of the order of the electroweak symmetry breaking scale. Its properties allow to perform stringent tests of the SM and to search for new physics through a deviation from SM predictions.

At the Tevatron center of mass energy top quarks are produced primarily in $t\bar{t}$ pairs via the strong process $p\bar{p} \rightarrow t\bar{t}$. In the SM each top quark decays through charged current weak interaction almost exclusively into a real W and a b quark ($t \rightarrow Wb$). Each W subsequently decays into either a charged lepton and a neutrino or two quarks. The $t\bar{t} \rightarrow W^+bW^-\bar{b}$ events can

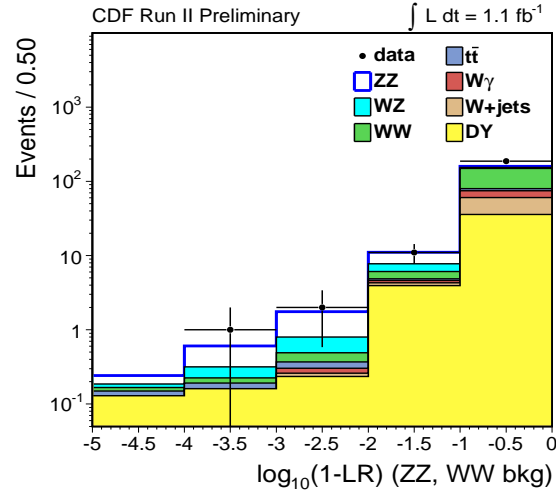


Fig. 7. Distribution of $\log(1-LR)$ for $ll\nu\nu$ candidate events used in ZZ cross section measurement.

thus be identified by means of different combinations of energetic leptons and jets. The branching ratio for both W 's from a $t\bar{t}$ pair to decay leptonically is: $2/81$ for $e\mu$, $e\tau$, $\mu\tau$ and $1/81$ for ee , $\mu\mu$, $\tau\tau$ (*dilepton channels*). Decay modes of $t\bar{t}$ pairs in which one W boson decays hadronically and the other leptonically into an e or a μ (*single lepton + jets channel*) have a branching ratio of $24/81$. When both W 's decay hadronically (*all hadronic channel*) the branching ratio is $36/81$. CDF and D0 identified top quark candidate events using most of these signatures.

8 Top Pair Cross Section Measurement

By measuring the $t\bar{t}$ production cross section $\sigma_{t\bar{t}}$ in many channels and comparing it to perturbative QCD calculations, we can test the SM predictions in great detail. The experimental uncertainty on the top quark pair production cross section has become comparable to the theoretical one ($\approx 12\%$) [15]. Figure 8 shows a summary of the top pair cross section measurements in the various channels at D0 (left plot) and CDF (right plot). All the measurements are consistent with each other and with the theoretical expectations, which are indicated by the vertical band.

D0 recently performed a simultaneous measurement of the $t\bar{t}$ production cross section and ratio $R = B(t \rightarrow Wb)/B(t \rightarrow Wq)$, counting the number of events with 0, 1 and at least 2 reconstructed b -quark jets (shown in figure 9). Figure 10 shows a summary of R measurements at the Tevatron. The measured $R = 0.991^{+0.094}_{-0.085}$ (stat+syst) can be translated into a lower limit on the V_{tb} Cabibbo-Kobayashi-Maskawa (CKM) matrix element of $|V_{tb}| > 0.901$ at 95% C.L. and assuming CKM unitarity.

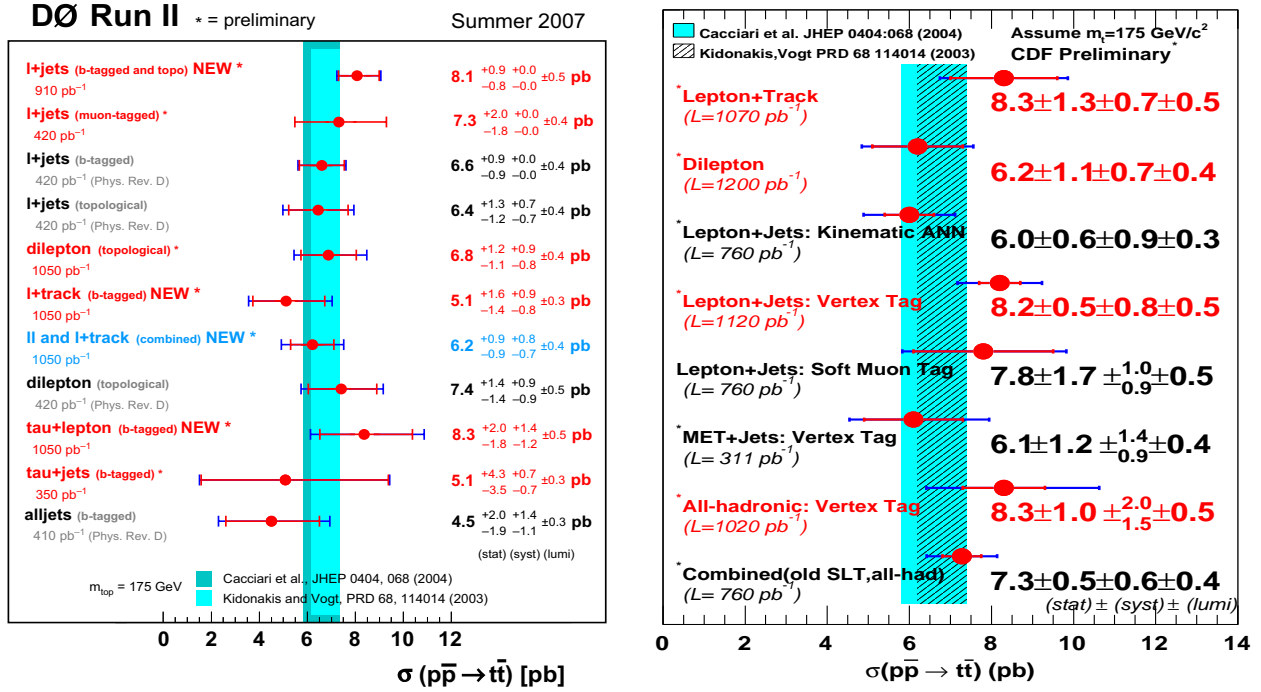


Fig. 8. A compilation of $t\bar{t}$ production cross section measurements at $\sqrt{s} = 1.96$ TeV for $M_{top} = 175$ GeV/ c^2 , performed by the D0 (left) and CDF (right) collaborations.

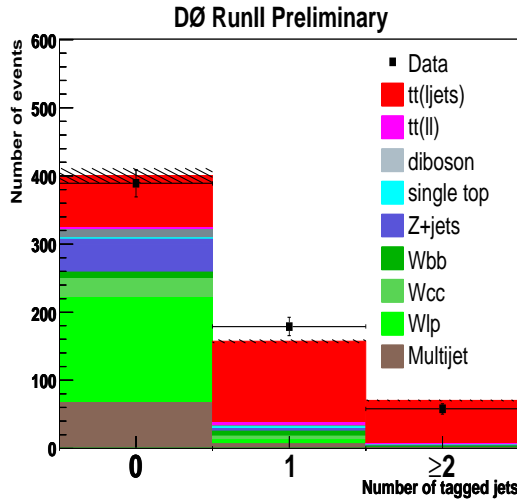


Fig. 9. Predicted and observed number of events in the zero, single and double b -tagged single lepton + jets samples, for top candidate events with at least four jets.

9 Top Mass Measurement

The top quark mass M_{top} is a fundamental parameter of the SM. Precise measurements of the top quark and W boson masses constraint the mass of the Higgs boson.

The reconstruction of the top quark mass presents several experimental challenges. The neutrinos from leptonically decaying W 's escape the detector. The quarks hadronize and form jets of particles whose energy must be corrected back to the parton level (the precision of the jet energy scale is crucial in this re-

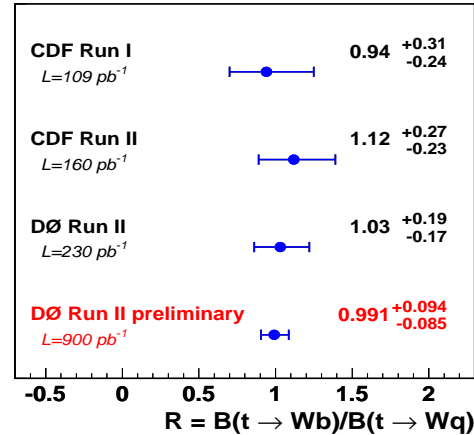


Fig. 10. Summary of $R = B(t \rightarrow Wb)/B(t \rightarrow Wq)$ measurements at the Tevatron

spect). The assignment of jets to partons usually has many possible permutations. Finally, there are background processes which mimic $t\bar{t}$ events.

CDF and D0 performed many determinations of M_{top} , using different techniques and all the top decay final states. In the single lepton + jets and all hadronic channels the uncertainty from jet energy scale (JES) can be reduced by using the reconstructed invariant dijet mass of the hadronically decaying W boson in top candidate events as an internal constraint (see Figure 11). This method converts the dominant systematic uncertainty into a statistical uncertainty, which will improve with more data.

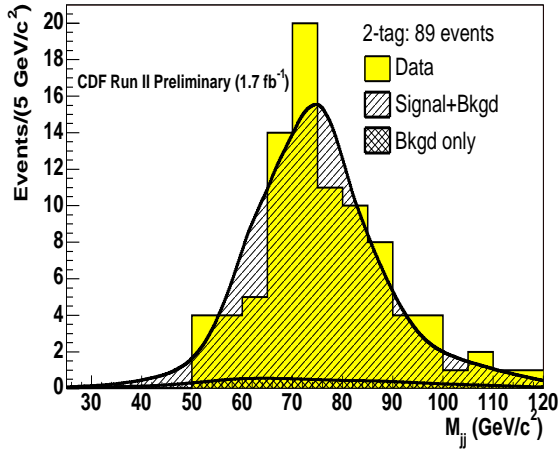


Fig. 11. Distribution of the reconstructed dijet mass from single lepton + jets top candidate events with two b tagged jets. A fit to signal and background templates is overlaid.

At the time of this writing, CDF obtained the most precise determination of the top mass in the single lepton + jets channel, using a matrix element integration method for the signal and a neural network discriminant to identify background events. CDF finds $M_{top} = 172.7 \pm 1.3$ (stat.) ± 1.2 (JES) ± 1.2 (syst) $\text{GeV}/c^2 = 172.7 \pm 2.1$ (total) GeV/c^2 , using 1.7 fb^{-1} of data. The precision of this single measurement is already better than the last combined CDF top mass result obtained using up to 1 fb^{-1} of data: $M_{top} = 170.5 \pm 2.2$ (total) GeV/c^2 .

D0 obtains its most precise top quark mass measurement by combining measurements performed in the dilepton, single lepton + jets and all hadronic channels. D0 finds: $M_{top} = 172.1 \pm 1.5$ (stat) ± 1.9 (syst) $\text{GeV}/c^2 = 172.1 \pm 2.4$ (total) GeV/c^2 , based on up to 1 fb^{-1} of data.

CDF obtained the best top mass measurement in the dilepton channel using the matrix element method and analyzing 1.8 fb^{-1} of data: $M_{top} = 170.4 \pm 3.1$ (stat.) ± 3.0 (syst) GeV/c^2 .

D0 recently presented a new top mass measurement in the dilepton channel based on 1 fb^{-1} of data, using two different weighting methods: $M_{top} = 173.7 \pm 5.4$ (stat.) ± 3.4 (syst) GeV/c^2 . Figure 12 shows a comparison between data and Monte Carlo of the peak mass for the 57 D0 dilepton top candidate events found in 1 fb^{-1} of data.

Figure 13 summarizes the most recent CDF and D0 top mass measurements and the Tevatron combined top mass result: $M_{top} = 170.9 \pm 1.1$ (stat) ± 1.5 (syst) $\text{GeV}/c^2 = 170.9 \pm 1.8$ (total) GeV/c^2 , based on data-sets including up to 1 fb^{-1} of data [16]. The top quark mass is known with a precision that was thought to be unreachable at the Tevatron only a few years ago: $\Delta M_{top}/M_{top} \approx 1.1\%$, of the order of the top natural width. Therefore, both experiments are now addressing a number of effects that, too small to have an impact on the previous measurements, could now

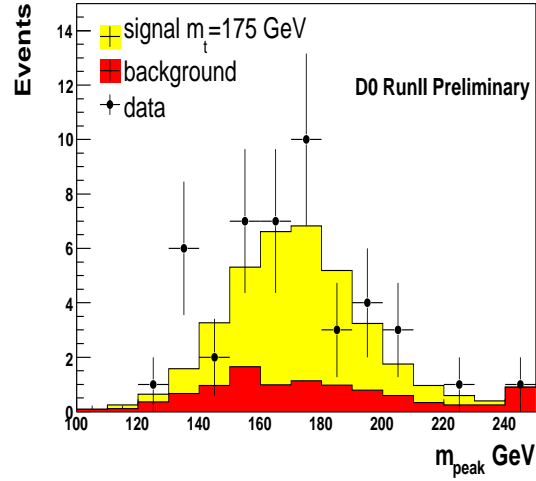


Fig. 12. Comparison of peak masses in data and Monte Carlo dilepton top candidate events.

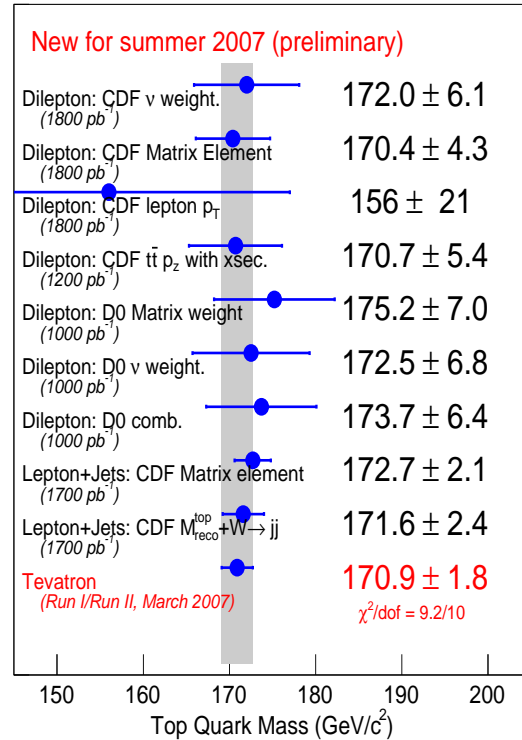


Fig. 13. A compilation of the most recent CDF and D0 top quark mass measurements and last Tevatron combined result.

become important. At the same time, they are figuring out which theoretical aspects are relevant, at the $1 \text{ GeV}/c^2$ level, and whether they are sufficiently well under control. Before the end of Run 2 the Tevatron experiments are likely to reach a $1 \text{ GeV}/c^2$ precision on the top quark mass.

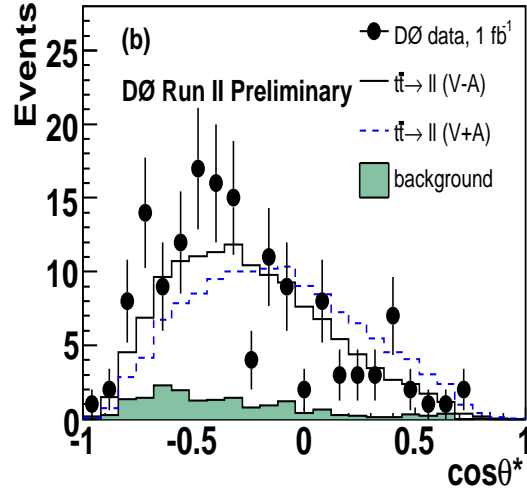


Fig. 14. $\cos \theta^*$ distribution observed in dilepton candidate events at D0. The SM prediction is shown as the solid line.

10 Top Quark Properties

After the top discovery phase, CDF and D0 moved to detailed studies of its properties. Both experiments investigated the top candidate events kinematic properties and the decay vertex. Among the many performed studies, here we show a very recent result on the W helicity in top decays. More results on top quark properties can be found in [17].

10.1 W Helicity in Top Decays

W helicity in top decays is fixed by the $V - A$ structure of the tWb vertex and it is reflected in the kinematics of W decay products. SM predicts that the fraction of left-handed W s is $F_- \approx 30\%$, the fraction of longitudinally polarized W s is $F_0 \approx 70\%$, while the right handed fraction F_+ is suppressed. Both experiments measure the angular distribution of charged leptons in the W rest frame measured with respect to the direction of motion of the W boson in the top-quark rest-frame ($\cos \theta^*$). Figure 14 and 15 show the $\cos \theta^*$ distributions observed in D0 dilepton and CDF single lepton + jets candidate events respectively.

Using 1 fb^{-1} of single lepton + jets and dilepton candidate events D0 measures $F_+ = 0.017 \pm 0.048(\text{stat}) \pm 0.047(\text{syst})$ ($F_+ < 0.14$ at 95% C.L.), with F_0 fixed to the SM value.

Using 1.7 fb^{-1} of single lepton + jets candidate events CDF measures $F_+ = 0.01 \pm 0.05(\text{stat}) \pm 0.03(\text{syst})$ ($F_+ < 0.12$ at 95% C.L.). CDF attempted also a 2 parameters fit, obtaining simultaneously both fractions: $F_0 = 0.38 \pm 0.22(\text{stat}) \pm 0.07(\text{syst})$ and $F_+ = 0.15 \pm 0.10(\text{stat}) \pm 0.04(\text{syst})$. Recently CDF presented a new analysis which measures $F_+ = -0.04 \pm 0.04(\text{stat}) \pm 0.03$ and therefore extracts a more stringent upper limit: $F_+ < 0.07$ at 95% C.L.. All results are consistent with SM predictions within the uncertainties.

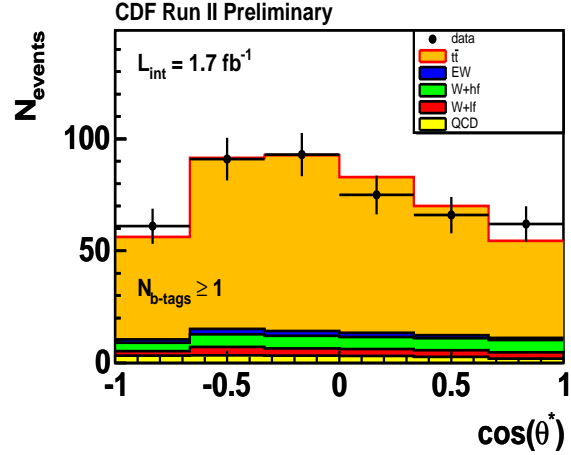


Fig. 15. The reconstructed $\cos \theta^*$ distribution observed in single lepton candidate events at CDF, together with the SM expectations.

11 Evidence for Single Top Production

The single top production mechanism involves electroweak production of a top quark via the Wtb vertex (t and s channel exchange of a virtual W boson). The experimental signature consists of the W decay products plus two or three jets, including one b quark jet from the decay of the top quark. In s -channel events a second b quark jet comes from the Wtb vertex. In t -channel events a second jet originates from the recoiling light-quark and a third low- E_T jet is produced at larger η through the splitting of the initial state gluon into a $b\bar{b}$ pair.

The production cross section is predicted to be 0.88 and 1.98 pb in the s and t channels respectively [18], about half than the pair production and with a much larger background. On the other hand, this mechanism allows a direct access to the V_{tb} CKM matrix element, and can be used to test the $V - A$ structure of the top charged current interaction.

In order to extract the single top signal from the challenging background dominated dataset, both experiments use various multi variate techniques. D0 presented the first evidence of single top quark production using 0.9 fb^{-1} of data [19]. D0 searched for single top with three analysis methods: decision trees (DT), matrix element (ME) and a neural network (NN). Discriminants are constructed with a large number of kinematic observables (DT, NN) or by evaluating the differential probability of signal using the single top ME. Combining the three analyses D0 finds a 3.6σ signal and measures a production cross section of 4.7 ± 1.3 pb. This can be translated into the first direct measurement of the V_{tb} CKM matrix element: $V_{tb} = 1.3 \pm 0.2$ (or $V_{tb}: 0.68 < |V_{tb}| < 1$ at 95% C.L.). Figure 16 shows the D0 results obtained with the three methods.

Recently CDF confirmed the evidence for single top production in 1.5 fb^{-1} of data, using a multivariate likelihood function technique (giving a 2.7σ excess over

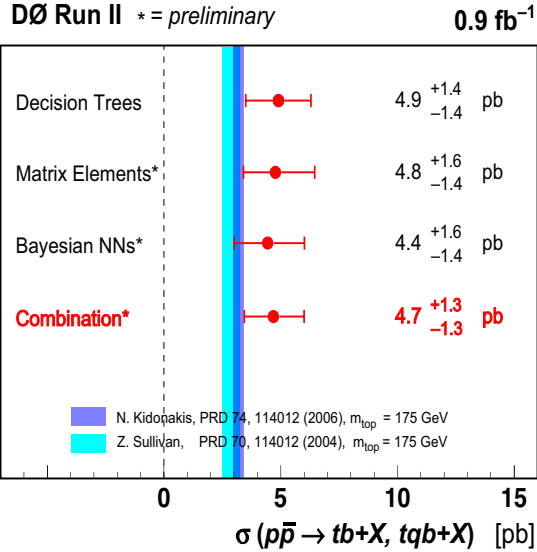


Fig. 16. DØ evidence for single top production.

the SM background) and a matrix element discriminant technique (giving a 3.1σ excess). CDF measures: $V_{tb} = 1.08 \pm 0.18$ (exp) ± 0.07 (theory).

12 Indirect Limits on Higgs Mass

The Higgs boson is the last remaining SM particle to be observed, and the one responsible for generating the W and Z boson masses. Direct searches at LEP experiments have excluded a Higgs boson with mass less than 114.4 GeV/ c^2 at 95% C.L. in the production mode $e^+e^- \rightarrow ZH$ [20]. The mass of the W depends on the top quark and Higgs masses through radiative effects. Since the Higgs mass is unknown, experimental measurements of the top and W boson masses provide the strongest indirect constraints on the Higgs mass, based on its contribution to the radiative correction which grows logarithmically with the Higgs mass at the one loop level. Figure 17 shows the SM prediction of M_W as a function of M_{top} for Higgs masses ranging from 114 to 1000 GeV/ c^2 . Figure 18 shows the $\Delta\chi^2$ curve derived from a global fit to precision electroweak measurements as a function of the Higgs-boson mass, assuming the SM to be the correct theory of nature. The preferred value for the Higgs mass, corresponding to the minimum of the curve, is $M_H = 76^{+33}_{-24}$ GeV/ c^2 , well below the lower experimental limit set by the LEP 2 experiments. The upper limit on M_H has been set at 144 GeV/ c^2 , at 95% C.L., and rises to 182 GeV/ c^2 if one takes into account the LEP 2 direct limit.

In the context of the minimal supersymmetric models (MSSM) the overall agreement of all observables appears very good for a wide region of the parameter space [21]. Figure 19 shows the $M_W - M_{top}$ plane prediction of the SM and the MSSM compared to the experimental result. The predictions within the two models consist of two bands with a small overlap region. The latter corresponds in the SM to a light Higgs bo-

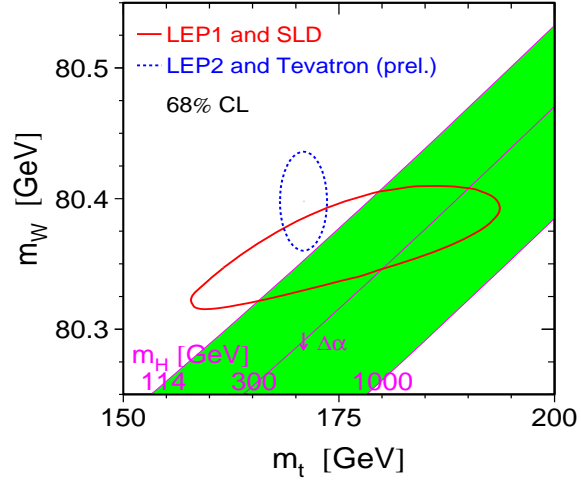


Fig. 17. Expectations for M_W as a function of M_{top} . The green diagonal band covers a wide range of Higgs-boson masses. The small ellipse represents the combination of LEP2 and Tevatron direct measurements.

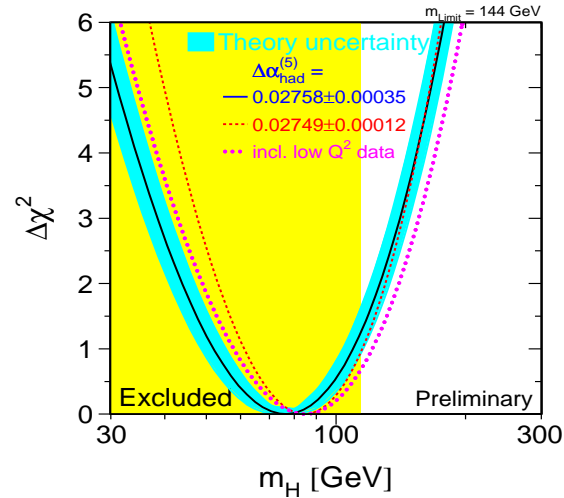


Fig. 18. $\Delta\chi^2$ curve as a function of the Higgs-boson mass. The minimum of the curve gives the preferred Higgs-boson mass.

son and in the MSSM to the parameters region where all superpartners are heavy. The current experimental measurements of M_W and M_{top} prefer a relatively light Higgs mass. Only by the end of Run 2 one might gather indirect information on the Higgs SUSY sector from the M_W and M_{top} measurements [21].

13 Conclusions

The Run 2 of the Tevatron is well underway. Tevatron experiments have in their hands a gold mine of more than 2 fb⁻¹ of data. Both CDF and DØ are producing

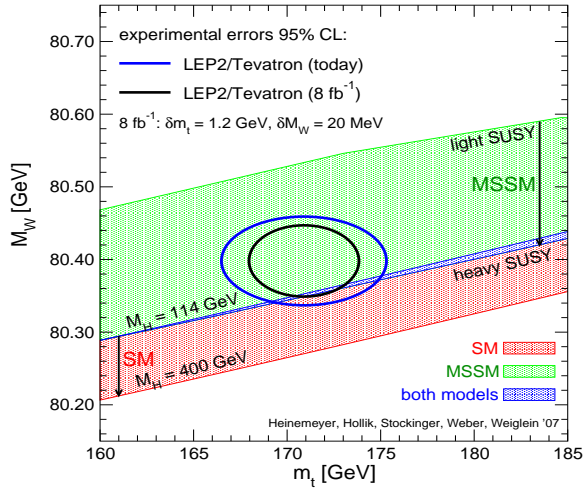


Fig. 19. Prediction for M_W in the SM and the MSSM as a function of M_{top} . The allowed MSSM band is obtained scanning over the SUSY mass parameters. The allowed SM band is obtained varying the M_H in SM. The two ellipses correspond to the present experimental situation at 95% C.L. and to the extrapolation assuming 8 fb^{-1} of data at the Tevatron.

interesting results in the electroweak sector, bringing SM tests to a level of precision which meets or exceed that of electron-positron colliders. The top quark mass is known with a 1.1% precision, the W boson mass with a 0.04% precision. They together limit the mass of the SM Higgs to be smaller than $144 \text{ GeV}/c^2$ at 95% C.L.. CDF and D0 will continue to collect data ($6\text{--}8 \text{ fb}^{-1}$ are expected by the end of Run 2) and to improve the precision on top and W masses over the next few years.

14 Acknowledgments

I would like to thank the SUSY07 organizers, for giving me the opportunity to give this presentation, and all of the CDF and D0 colleagues, who made possible to have these high quality physics results. In particular, my thanks to T. Bolton, G. Chiarelli, R. Erbacher, E. Halkiadakis, C. Hays, E. James, E. Shabalina, K. Tollefson, W. Wagner for their help and suggestions in preparing this talk and paper.

References

1. T. Lecompte and H.T. Diehl, Ann. Rev. Nucl. Part. Sci. **50** (2000) 71.
2. D. Acosta *et al.* (CDF Collaboration), Phys. Rev. Lett. **94**, (2005) 091803; A. Abulencia *et al.* (CDF Collaboration), Phys. Rev. D **75**, (2007) 092004; V.M. Abazov *et al.* (D0 Collaboration), Phys. Rev. D **71**, (2005) 072004; D0 Conf. Note 4750; D0 conf. note 4403.
3. C. Anastasiou *et al.*, Phys. Rev. D **69**, (2004) 094008.
4. A. Abulencia *et al.* (CDF Collaboration), Phys. Rev. Lett. **98**, (2007) 251801.

5. T. Aaltonen *et al.* (CDF Collaboration), Phys. Rev. Lett. **99**, (2007) 151801; T. Aaltonen *et al.* (CDF Collaboration), arXiv:0708.3642v1 (2007), submitted to Phys. Rev. D.
6. The LEP Electroweak Working Group, <http://lepewwg.web.cern.ch/LEPEWWG/>
7. T. Aaltonen *et al.* (CDF Collaboration), arXiv:0710.4112 (2007), submitted to Phys. Rev. Lett.
8. D. Acosta *et al.* (CDF Collaboration), Phys. Rev. D **71**, (2005) 061104; V.M. Abazov *et al.* (D0 Collaboration), arXiv:0709.4254v1, submitted to Phys. Rev. D.
9. V.M. Abazov *et al.* (D0 Collaboration), Phys. Rev. Lett. **94**, (2005) 151801; D. Acosta *et al.* (CDF Collaboration), Phys. Rev. Lett. **94**, (2005) 211801.
10. D. Acosta *et al.* (CDF Collaboration), Phys. Rev. Lett. **94**, (2005) 041803; V.M. Abazov *et al.* (D0 Collaboration), Phys. Lett. B **653**, (2007) 378.
11. J.M. Campbell and R.K. Ellis, Phys. Rev. D **60**, (1999) 113006.
12. V. M. Abazov *et al.* (D0 Collaboration), arXiv:0709.2917v1, submitted to Phys. Rev. D.
13. A. Abulencia *et al.* (CDF Collaboration), Phys. Rev. Lett. **98**, (2007) 161801.
14. F. Abe *et al.* (CDF Collaboration), Phys. Rev. Lett. **74**, (1995) 2626; S. Abachi *et al.* (D0 Collaboration), Phys. Rev. Lett. **74**, (1995) 2632.
15. M. Cacciari *et al.*, JHEP **0404**, (2004) 068; N. Kidonakis, Int. J. Mod. Phys. A **19**, (2004) 1793.
16. Tevatron electroweak working group, arXiv:hep-ex/0703034v1.
17. S. Cabrera, this proceedings.
18. Z. Sullivan, Phys. Rev. D **70**, (2004) 114012.
19. V.M. Abazov *et al.* (D0 Collaboration), Phys. Rev. Lett. **98**, (2007) 181802.
20. R. Barate *et al.*, Phys. Lett. B **565**, (2003) 61.
21. S. Heinemeyer, W. Hollik, D. Stockinger, A.M. Weber and G. Weiglein, JHEP **08** (2006) 052.